

Spin dynamics in NaFeAs and NaFe_{0.53}Cu_{0.47}As probed by resonant inelastic X-ray scattering

Yu Song,^{1,2,*} Weiyi Wang,¹ Eugenio Paris,³ Xingye Lu,^{4,3} Jonathan Pellicciari,^{3,†}
Yi Tseng,³ Yaobo Huang,³ Daniel McNally,³ Marcus Dantz,³ Chongde Cao,⁵
Rong Yu,⁶ Robert J. Birgeneau,² Thorsten Schmitt,³ and Pengcheng Dai^{1,‡}

¹*Department of Physics and Astronomy, Rice University, Houston, Texas 77005, USA*

²*Department of Physics, University of California, Berkeley, California 94720, USA*

³*Photon Science Division, Swiss Light Source, Paul Scherrer Institut, 5232 Villigen PSI, Switzerland*

⁴*Center for Advanced Quantum Studies and Department of Physics,
Beijing Normal University, Beijing 100875, China*

⁵*MOE Key Laboratory of Materials Physics and Chemistry under Extraordinary
Conditions and Shaanxi Key Laboratory of Condensed Matter Structures and Properties,
School of Physical Science and Technology, Northwestern Polytechnical University, Xian 710072, China*

⁶*Department of Physics and Beijing Key Laboratory of Opto-electronic Functional Materials and Micro-nano Devices,
Renmin University of China, Beijing 100872, China*

The parent compounds of iron-based superconductors are magnetically-ordered bad metals, with superconductivity appearing near a putative magnetic quantum critical point. The presence of both Hubbard repulsion and Hund's coupling leads to rich physics in these multiorbital systems, and motivated descriptions of magnetism in terms of itinerant electrons or localized spins. The NaFe_{1-x}Cu_xAs series consists of magnetically-ordered bad metal ($x = 0$), superconducting ($x \approx 0.02$) and magnetically-ordered semiconducting/insulating ($x \approx 0.5$) phases, providing a platform to investigate the connection between superconductivity, magnetism and electronic correlations. Here we use X-ray absorption spectroscopy and resonant inelastic X-ray scattering to study the valence state of Fe and spin dynamics in two NaFe_{1-x}Cu_xAs compounds ($x = 0$ and 0.47). We find that magnetism in both compounds arises from Fe²⁺ atoms, and exhibits underdamped dispersive spin waves in their respective ordered states. The dispersion of spin excitations in NaFe_{0.53}Cu_{0.47}As is consistent with being quasi-one-dimensional. Compared to NaFeAs, the band top of spin waves in NaFe_{0.53}Cu_{0.47}As is slightly softened with significantly more spectral weight of the spin excitations. Our results indicate the spin dynamics in NaFe_{0.53}Cu_{0.47}As arise from localized magnetic moments and suggest the iron-based superconductors are proximate to a correlated insulating state with localized iron moments.

PACS numbers: 74.25.Ha, 74.70.-b, 78.70.Nx

I. INTRODUCTION

The parent compounds of cuprate superconductors are magnetically-ordered Mott-insulators, where the spin-1/2 Cu²⁺ moments forming antiferromagnetic (AF) order are completely localized and can be well-described by a Heisenberg Hamiltonian [1–3]. Because high-temperature superconductivity in cuprates is derived from magnetically-ordered parent compounds after eliminating static AF order, it is generally believed that electronic correlations and magnetism are important for the superconductivity of these materials [1, 2]. Spin dynamics in the parent compounds of cuprate superconductors are described by spin waves due to interactions between localized moments [3]. Cuprate superconductors ex-

hibit similar spin dynamics, especially in the underdoped regime and at high-energies, suggesting the inheritance of short-range spin correlations from their parent compounds [4–7]. In contrast, the parent compounds of iron-based superconductors (FeSCs) are magnetically-ordered bad metals with significant electronic correlations [8–11], suggesting that their spin dynamics may originate from either localized spins or itinerant electrons.

In contrast to the cuprates which can be effectively described using a single orbital, the FeSCs are multiorbital systems (with five $3d$ orbitals), and the presence of both Hubbard repulsion U and Hund's coupling J_H leads to a rich theoretical phase diagram [10, 11]. At half-filling (with a total of $n = 5$ electrons per Fe), both U and J_H promote a Mott insulating state. Away from half-filling (such as $n = 6$), while large U and J_H lead to strong electronic correlations, a bad-metal state becomes favorable and a Mott insulating state is realized only for an intermediate range of J_H [12, 13].

Since parent compounds of the FeSCs (with $n = 6$) exhibit large values of resistivity, comparable to those of underdoped cuprates, they fall in the bad metal regime, and have been suggested to exhibit incipient Mott physics [14]. In such a scenario, the metallic transport is due

*Current affiliation: Department of Physics, Zhejiang University, Hangzhou 310027, China; Electronic address: yusong.phys@zju.edu.cn

†Current affiliation: National Synchrotron Light Source-II, Brookhaven National Laboratory, Upton, NY 11973, USA

‡Electronic address: pdai@rice.edu

to the coherent part of the single-electronic excitations, while magnetism results from localized moments formed by the incoherent part [11]. From this perspective, as electronic correlations are enhanced, a magnetically-ordered $n = 6$ insulating phase should appear. BaFe_2Se_3 and BaFe_2S_3 tuned via pressure may be a realization of such a scenario [15–18], with their ground states transformed from magnetically-ordered insulators under ambient conditions to superconductivity under pressure (the strength of electronic correlations decreases with increasing pressure). Alternatively, the FeSCs may be anchored around a half-filled ($n = 5$) Mott insulating state, with the magnetic and nematic orders in the parent compounds ($n = 6$) being the competing states that suppress superconductivity [19].

As an archetypal parent compound of FeSCs, NaFeAs exhibits a tetragonal-to-orthorhombic transition below $T_S \approx 55$ K and stripe-type collinear magnetic order [Fig. 1(a)] below $T_N \approx 45$ K [20–22]. The magnetic and structural phase transitions in NaFeAs are quickly suppressed upon Cu-doping, giving way to superconductivity near $x \approx 0.02$ [23]. With further increase of Cu concentration, $\text{NaFe}_{1-x}\text{Cu}_x\text{As}$ starts to exhibit semiconducting/insulating electrical transport, accompanied by the appearance of short-range magnetic order and charge-gapped patches [24, 25]. Upon approaching $x = 0.5$, Fe and Cu order into stripes and long-range magnetic order with $T_N \approx 200$ K reemerges [Fig. 1(b)], accompanied by a charge gap that persists above T_N [25–28]. The ordering between Fe and Cu atoms in the $x = 0.5$ compound is a structural analogue of the stripe-type magnetic order in NaFeAs , resulting in quasi-one-dimensional (quasi-1D) Fe chains separated by nonmagnetic Cu chains. Such a superstructure has been suggested to be essential for the insulating properties [29] and the electronic structure [30] of the $x = 0.5$ compound. The magnetic structure of $\text{NaFe}_{0.5}\text{Cu}_{0.5}\text{As}$ can be obtained from that of NaFeAs simply by replacing half of Fe atoms by nonmagnetic Cu atoms and rotating the orientations of magnetic moments by 90° , although with a much larger ordered moment ($\geq 1.1 \mu_B/\text{Fe}$ [25]) relative to that of NaFeAs ($\sim 0.1 \mu_B/\text{Fe}$ [20–22]). Locally, while the Fe-As distance is slightly larger in $\text{NaFe}_{0.5}\text{Cu}_{0.5}\text{As}$ compared to NaFeAs , the heights of As atoms away from the transition metal planes are similar in the two compounds [Figs. 1(c) and (d)]. While simple valence counting suggests Fe to be in a $3+$ state with $n = 5$ [25], the similar local environments of Fe ions in NaFeAs and $\text{NaFe}_{0.5}\text{Cu}_{0.5}\text{As}$ suggests Fe in the latter to be in a $2+$ state with $n = 6$.

Near $x \approx 0.5$, the insulating/semiconducting electrical transport in $\text{NaFe}_{1-x}\text{Cu}_x\text{As}$ exhibits a low-temperature resistivity $\sim 1 \Omega \cdot \text{cm}$. Such a resistivity value is comparable to that found in $\text{Fe}_{1+\delta-x}\text{Cu}_x\text{Te}$ ($0.1\text{--}1 \Omega \cdot \text{cm}$ when $x \approx 0.5$) [31–34], but contrasts with the much smaller resistivity values ($\sim 1 \text{ m}\Omega \cdot \text{cm}$) in the $\text{Sr}(\text{Fe}_{1-x}\text{Cu}_x)_2\text{As}_2$ [35] and $\text{Ba}(\text{Fe}_{1-x}\text{Cu}_x)_2\text{As}_2$ [36] series. Such a difference may result from stronger electronic correlations in NaFeAs and FeTe [9, 37], which persist upon $\sim 50\%$ Cu-

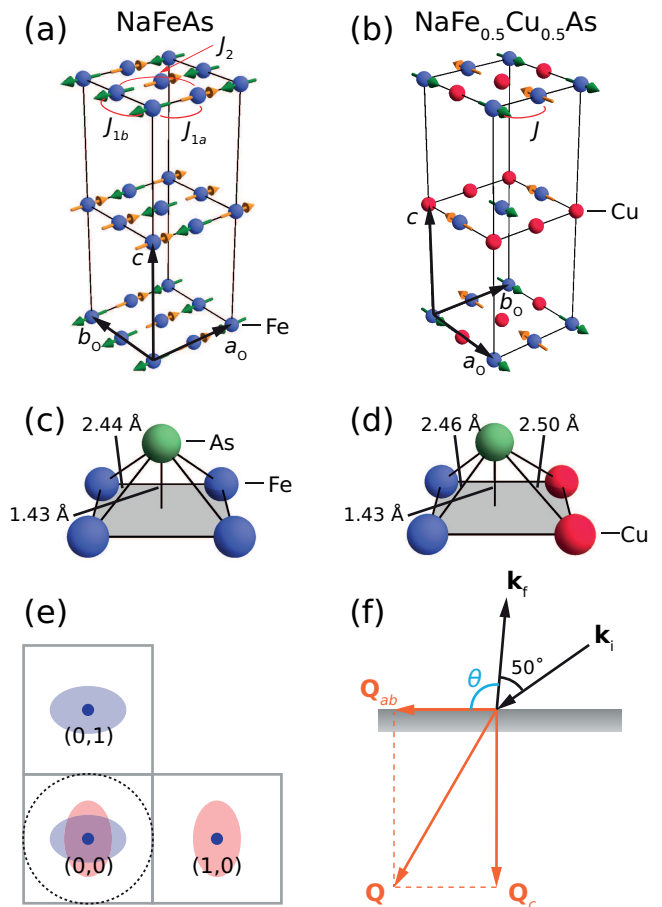


Figure 1: (a) Magnetic structure of NaFeAs . (b) Magnetic structure of $\text{NaFe}_{0.5}\text{Cu}_{0.5}\text{As}$. (c) Local atomic environment in NaFeAs , with atomic distances from Ref. [20] for $T = 295$ K. (d) Local atomic environment in $\text{NaFe}_{0.5}\text{Cu}_{0.5}\text{As}$, with atomic distances from Ref. [25] for $T = 250$ K. (e) Reciprocal space of NaFeAs and $\text{NaFe}_{0.5}\text{Cu}_{0.5}\text{As}$. In both cases two types of domains are present, with spin waves exhibiting intensities at either $\mathbf{Q} = (1, 0)$ or $\mathbf{Q} = (0, 1)$. Since the reciprocal space probed by RIXS is limited to the dashed circle near $\mathbf{Q} = (0, 0)$ for NaFeAs (2% larger in diameter for $\text{NaFe}_{0.5}\text{Cu}_{0.5}\text{As}$), intensities from twin domains overlap. The shaded ellipsoids are schematic intensity contours for spin waves with anisotropic spin velocities in NaFeAs and $\text{NaFe}_{0.5}\text{Cu}_{0.5}\text{As}$. (f) Schematic scattering geometry of our RIXS measurements.

doping and cause these systems to exhibit larger resistivity values. Another possibility is that while the structure of $\text{Sr}(\text{Fe}_{1-x}\text{Cu}_x)_2\text{As}_2$ and $\text{Ba}(\text{Fe}_{1-x}\text{Cu}_x)_2\text{As}_2$ allows the formation of c -axis collapsed phases with As-As covalent bonds [38, 39], such a phase is unlikely in $\text{NaFe}_{1-x}\text{Cu}_x\text{As}$ and $\text{Fe}_{1+\delta-x}\text{Cu}_x\text{Te}$. From a theoretical perspective, insulating/semiconducting $\text{NaFe}_{1-x}\text{Cu}_x\text{As}$ with $x \approx 0.5$ may be a Mott insulator [25], in which an electronic gap opens due to strong electron-electron interactions; alternatively, a Slater insulator scenario, in which an electronic gap results from the symmetry lowering associated with magnetic order, has also been suggested [27]. In the latter

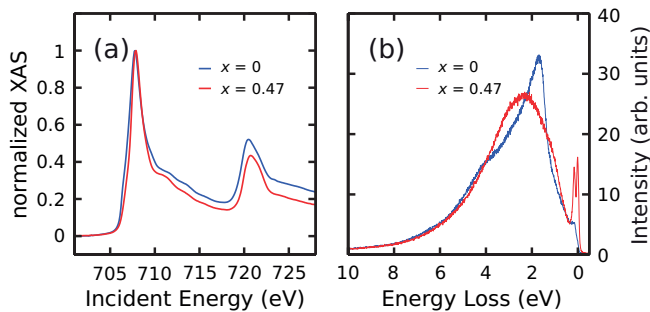


Figure 2: (Color online) (a) X-ray absorption spectroscopy measurements for $\text{NaFe}_{1-x}\text{Cu}_x\text{As}$ for $x = 0$ and $x = 0.47$. The measured spectra have been normalized so that the intensity maximum (minimum) corresponds to 1 (0). (b) Typical RIXS spectra compared for $x = 0$ ($\mathbf{Q}_{ab} = (0.50, 0)$) and $x = 0.47$ ($\mathbf{Q}_{ab} = (0.51, 0)$) samples. All RIXS spectra are normalized by integrated intensity within the energy loss range $[0.4, 10]$ eV.

scenario, persistent insulating/semiconducting above T_N is suggested to result from spin fluctuations that persist well above T_N in a quasi-1D system, which lead to an electronic gap similar to static magnetic order.

Spin dynamics in the FeSCs not only contain information on their magnetic interactions, but also provide clues regarding the size of the fluctuating magnetic moment (seen within timescale of the experimental probe), which in turn reflects the system's degree of itinerancy/localization [40–42]. While spin dynamics in FeSCs and related compounds are typically investigated using inelastic neutron scattering (INS) [42–44], resonant inelastic X-ray scattering (RIXS) has emerged as a useful complementary probe [45–55]. Since NaFeAs and $\text{NaFe}_{0.5}\text{Cu}_{0.5}\text{As}$ exhibit significant similarities in their crystal and magnetic structures, a comparison of the spin dynamics in the two systems may provide insights for understanding the magnetism in the FeSCs.

In this work, we use X-ray absorption spectroscopy (XAS) and RIXS to study magnetically ordered $\text{NaFe}_{1-x}\text{Cu}_x\text{As}$ with $x = 0$ and 0.47 [Figs. 1(a) and (b)]. Our XAS measurements reveal that Fe atoms maintain a +2 valence in both compounds, despite Cu being in a +1 state in the latter. Underdamped dispersive spin waves were uncovered in both compounds, consistent with their magnetically ordered ground states. Measurements along the (q, q) direction is unaffected by twinning and allows the intrinsic spin wave dispersion to be extracted through RIXS measurements. Compared to spin waves in NaFeAs, the spin waves in $\text{NaFe}_{0.53}\text{Cu}_{0.47}\text{As}$ are softer in energy but more intense in intensity, indicating a larger total (ordered and fluctuating) moment and stronger electronic correlations associated with its Fe^{2+} state. Our results suggest the magnetism in $\text{NaFe}_{0.5}\text{Cu}_{0.5}\text{As}$ arises from localized spins, and are consistent with the FeSCs being close to a $n = 6$ correlated insulating state.

II. METHODS

A. Experimental Details

Single crystals of $\text{NaFe}_{1-x}\text{Cu}_x\text{As}$ ($x = 0$ and 0.47) were grown using the self-flux method [23, 25]. We probe the spin dynamics in the $x = 0.47$ sample to approximate the ideal $\text{NaFe}_{0.5}\text{Cu}_{0.5}\text{As}$ system. RIXS measurements were carried out using the ADDRESS beamline at the Swiss Light Source, Paul Scherrer Institute [56, 57]. The instrument energy resolution was calibrated using carbon tape and can be well-described by a pseudo-Voigt form, with a width (FWHM) of ≈ 86 meV. Since NaFeAs and its doped variants are highly air-sensitive, all sample preparations and transfers were carried out under either Ar or N_2 flow. Atomically flat pristine surfaces were then post-cleaved inside the chamber under ultra-high vacuum. Momentum transfers are labeled in reciprocal lattice units, using the orthorhombic unit cell [Figs. 1(a) and (b)] with $a \approx b \approx 5.59$ Å, $c \approx 6.97$ Å for $x = 0$ and $a \approx b \approx 5.70$ Å, $c \approx 6.88$ Å for $x = 0.47$. Samples were aligned in either (H, H, L) or $(H, 0, L)$ scattering planes. We used a fixed scattering angle of 130° , with grazing incident beam predominantly in the ab -plane of the sample and linearly polarized in the scattering plane (π polarized). The fixed scattering angle results in a fixed total momentum transfer \mathbf{Q} , while the in-plane (\mathbf{Q}_{ab}) and out-of-plane (\mathbf{Q}_c) components can be varied by rotating the sample with respect to the incident beam [Fig. 1(f)]. The accessible range of \mathbf{Q}_{ab} is limited by kinematic constraints [Fig. 1(e)], and the layered nature of $\text{NaFe}_{1-x}\text{Cu}_x\text{As}$ samples suggest their spin dynamics have minimal dependence on \mathbf{Q}_c (for example a dispersion of only a few meV along \mathbf{Q}_c is seen for NaFeAs [58]). RIXS spectra were collected at the Fe L_3 -edge ($E_i = 707.9$ eV). All measurements were carried out at $T = 17$ K, well inside the magnetically ordered state of both NaFeAs ($T_N \approx 45$ K [20, 21]) and $\text{NaFe}_{0.53}\text{Cu}_{0.47}\text{As}$ ($T_N \approx 200$ K [25]). The detector used has a pixel density of ≈ 30.8 meV/pixel (with a subpixeling of 4 we have ≈ 7.7 meV/subpixel), providing a significantly finer sampling of the RIXS spectra compared to previous work on $\text{NaFe}_{1-x}\text{Co}_x\text{As}$ [49] with ≈ 50 meV/pixel.

Structural twinning common to the FeSCs with low-temperature orthorhombic lattice structures is expected in both measured samples. In the magnetically-ordered state of NaFeAs, there are magnetic domains that have antiferromagnetic spin stripes running along the $(q, 0)$ or the $(0, q)$ direction, corresponding to domains that order magnetically at the $(1, 0)$ and $(0, 1)$ positions, respectively. Similarly, in $\text{NaFe}_{0.53}\text{Cu}_{0.47}\text{As}$, there are domains with Fe chains that run along the $(q, 0)$ or $(0, q)$ direction, also resulting in magnetic order at the $(1, 0)$ and $(0, 1)$ positions, respectively. While the magnetic ordering vectors associated with the two types of domains are separate in momentum space, spin excitations stemming from $(0, 0)$ inevitably overlap (Fig. 1(e)). Therefore, due to twinning, our data measured along the $(q, 0)$ direction

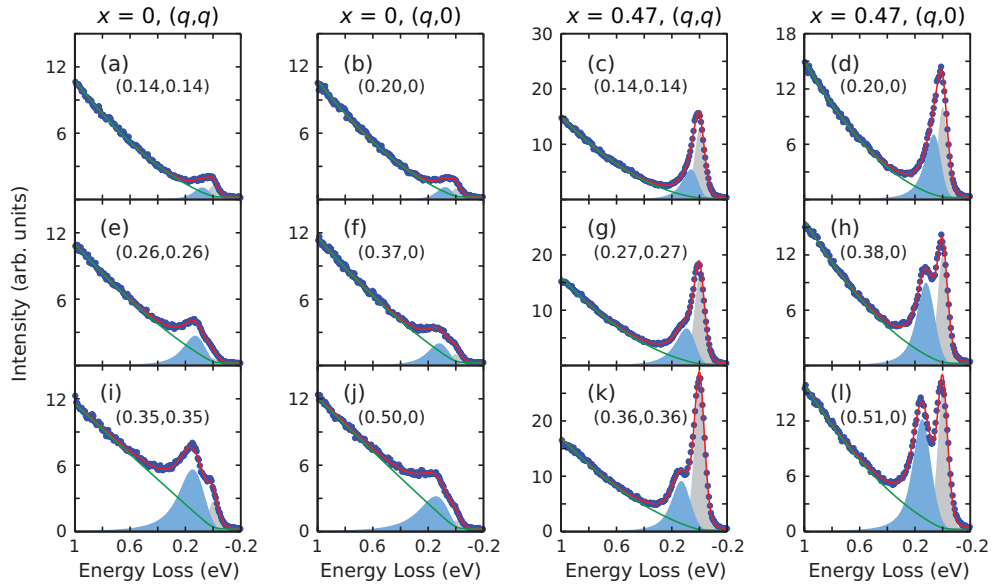


Figure 3: (Color online) RIXS spectra for $\text{NaFe}_{1-x}\text{Cu}_x\text{As}$ with $x = 0$ and $x = 0.47$. Each column of plots corresponds to measurements done for either $x = 0$ or $x = 0.47$, and for \mathbf{Q}_{ab} along either $(q, 0)$ or (q, q) . \mathbf{Q}_{ab} is labeled inside each panel. In each panel the measured data points (blue symbols), total fit intensity I_{total} (red line), $I_{\text{bkg}} + I_{\text{fluo}}$ (green line), I_{spin} (light blue shaded area), and the elastic peak (light gray shaded area) are presented.

contain contributions from both the $(H, 0)$ and $(0, K)$ directions of a single-domain sample. We note that because each measurement at a particular momentum position is obtained by binning multiple scans taken at randomly selected sample positions, even if structural domain sizes are larger than our beam spot, it remains reasonable to assume that the two domain types contribute similarly to our data. On the other hand, twinning does not affect measurements along the (q, q) direction (Fig. 1(e)).

B. Data Analysis

To avoid beam damage, each measurement is repeated multiple times by translating the sample so that no single position is irradiated for more than 5 minutes. The repeated scans are combined and then normalized to their integrated intensity in the energy loss range $[0.4, 10]$ eV, which is dominated by the fluorescence signal, with intensity proportional to the amount of Fe atoms probed in the measurement. Within the energy loss range $[-1, 1]$ eV, we modeled the RIXS spectra (I_{total} as a function of energy loss E) with a linear background (I_{bkg}), an elastic peak ($c\delta(E)$), a fluorescence signal (I_{fluo}) and spin excitations (I_{spin}):

$$I_{\text{total}}(E) = I_{\text{bkg}}(E) + c\delta(E) + I_{\text{fluo}}(E) + I_{\text{spin}}(E). \quad (1)$$

The background I_{bkg} is modeled as a linear function. The fluorescence is modeled as a second-order polynomial:

$$I_{\text{fluo}}(E) = (p_1 E + p_2 E^2)H(E), \quad (2)$$

with $H(E)$ being the Heaviside step function. For consistency, we used the same model to describe the fluorescence for both $x = 0$ and $x = 0.47$ samples, even though the ground state of $\text{NaFe}_{1-x}\text{Cu}_x\text{As}$ with $x \approx 0.5$ exhibits an electronic gap ~ 100 meV [26, 27]. We have carried out additional analysis to show that our conclusions are robust when I_{fluo} is modified to:

$$I_{\text{fluo}}(E) = [p_1(E - \Delta) + p_2(E - \Delta)^2]H(E - \Delta), \quad (3)$$

with $\Delta = 0.1$ or 0.2 eV (see the Appendix).

The spin excitations are described by a general damped harmonic oscillator function [59]:

$$I_{\text{spin}}(E) = \frac{A}{\pi} \frac{1}{1 - e^{-\beta E}} \frac{2\gamma E E_0}{(E^2 - E_0^2)^2 + (\gamma E)^2}, \quad (4)$$

which in the limit of no damping ($\gamma \rightarrow 0$) and low temperature ($\beta E \gg 1$) is $I_{\text{spin}} = A\delta(E - E_0)$. In addition, the position of zero energy loss ($E = 0$) is also set as a free parameter in our model. The measured RIXS spectra were then fit to our model of I_{total} , after convolving with the instrument energy resolution. We then extracted the values and uncertainties (1 s.d.) of the best fit parameters. It should be noted that fit values of E_0 and the zero energy position are correlated, so that the uncertainties obtained from fitting may be underestimated. This is especially the case for small in-plane momentum transfers, for which the spin excitations and the elastic line

strongly overlap, causing the fit values of E_0 to be overestimated and the associated fit uncertainties of E_0 to be underestimated.

C. $U(1)$ Slave-Spin Mean Field Theory

To understand the nature of the insulating behavior, we studied the multi-orbital Hubbard model for $\text{NaFe}_{0.5}\text{Cu}_{0.5}\text{As}$ using the $U(1)$ slave-spin theory [60]. Since Cu ions exhibit +1 valence and are nonmagnetic [25], the local (ionization) potential difference between the Fe and Cu ions is large and will suppress the hopping integral between Fe and Cu sites. This allows us to treat Cu ions in $\text{NaFe}_{0.5}\text{Cu}_{0.5}\text{As}$ as vacancies, with Fe atoms ordering into the quasi-1D chains as shown in Fig. 1(b). For the hopping parameters between Fe ions, we use those for NaFeAs [61]. In the calculation, the electron density is fixed to $n = 6$ per Fe ion, to be consistent with the observed +2 valence of Fe. The details of this method is presented in Ref. [60]. To study the metal-to-insulator transition of the model, we calculated the quasiparticle spectral weight, Z_α , in each Fe $3d$ orbital α . The ground state of the system is a Mott insulator if $Z_\alpha = 0$ in all orbitals, and is a metal if $Z_\alpha > 0$ for all orbitals. We have also found an orbital-selective Mott phase (OSMP), corresponding to $Z = 0$ in the d_{xy} orbital, and $Z_\alpha > 0$ for other orbitals. The resulting phase diagram is shown in Fig. 7.

III. RESULTS

A. X-ray absorption spectroscopy

XAS near the Fe L_3 -edge measured in total fluorescence yield (TFY) are compared for $\text{NaFe}_{1-x}\text{Cu}_x\text{As}$ ($x = 0$ and $x = 0.47$) in Fig. 2(a), after normalizing the spectra so that the maximum and minimum intensities respectively correspond to 1 and 0. Both spectra are dominated by an absorption peak at $E = 707.9$ eV, without an additional peak at $E \approx 710$ eV [62]. This suggests that Fe ions are in the Fe^{2+} state for both compounds, with minimal contributions from the Fe^{3+} state. This conclusion is surprising for the $x = 0.47$ compound, as Cu ions are in the Cu^{1+} state (see Supplementary Information of Ref. [25]) and valence counting suggests Fe ions to be in the Fe^{3+} state, when As ions are assumed to be in the As^{-3} state. Since As-As covalent bonding found in c -axis collapsed iron pnictides [39] is unlikely for the NaFeAs structure, this suggests that nominally the As ions may be in an unusual $\text{As}^{-2.5}$ state. At present, it is difficult to probe directly the valence state of As. The absorption peak at $E = 707.9$ eV is slightly sharper for the $x = 0.47$ sample compared to $x = 0$, which is a result of its more localized nature.

B. Resonant inelastic X-ray scattering

Since Fe ions are in the Fe^{2+} ($3d^6$) state for both NaFeAs and $\text{NaFe}_{0.53}\text{Cu}_{0.47}\text{As}$, in the RIXS process the electronic configuration of the Fe ions are excited from $2P_{3/2}^4 3d^6$ to $2P_{3/2}^3 3d^7$, and then relax back to $2P_{3/2}^4 3d^6$, allowing for the creation of spin excitations with $\Delta S = 1$. Fig. 2(b) compares representative RIXS spectra for the $x = 0$ ($\mathbf{Q}_{ab} = (0.50, 0)$) and 0.47 ($\mathbf{Q}_{ab} = (0.51, 0)$) samples over a broad energy transfer range. As can be seen, broad fluorescence peaks are seen for both samples. The presence of clear differences indicates a significant modification of the electronic structure upon heavy Cu-substitution in NaFeAs [25–27, 29]. For energies less than 0.5 eV, an additional inelastic peak can be resolved, which can be attributed to spin excitations. The intensity of this feature is more prominent in the $x = 0.47$ sample, with the RIXS spectra normalized to integrated intensity in the energy loss range [0.4, 10] eV. This suggests that the spectral weight of spin excitations per Fe atom is substantially larger in the $x = 0.47$ compound. The elastic peak is also more prominent in the $x = 0.47$ sample, which is likely caused by stronger Laue monotonic scattering [63] due to increased disorder.

To focus on the spin dynamics, we analyzed our RIXS data within an energy window of $[-1, 1]$ eV, with representative scans and the corresponding fits summarized in Fig. 3. The green solid lines represent the results of fits to the fluorescence on top of a linear background ($I_{\text{bkg}} + I_{\text{fluo}}$), and the shaded areas are either damped harmonic oscillators that capture the spin excitations (I_{spin}) or elastic peaks. As can be seen, all scans are well-described by our model of I_{total} , allowing the intensity of the spin excitations I_{spin} to be separated. Fig. 8 in the Appendix shows a comparison between data and fit I_{spin} after the fit background, elastic peak, and fluorescence have been subtracted.

Since our data are normalized using the fluorescence peak, it is meaningful to compare quantitatively the intensity of spin excitations as a function of \mathbf{Q}_{ab} and doping x . Color-coded and interpolated intensities of spin excitations for the $x = 0$ and 0.47 samples are compared in Fig. 4. Overall, the spin excitations appear more intense in the $x = 0.47$ sample (note the different color scales in panels (a)-(b) compared to (c)-(d)). A quantitative comparison of the spin excitation intensities is presented in Fig. 5(c), through the fit parameter A ($I_{\text{spin}} = A\delta(E - E_0)$ as $\gamma \rightarrow 0$). As can be seen, spin excitations are clearly more intense in $\text{NaFe}_{0.53}\text{Cu}_{0.47}\text{As}$ compared to NaFeAs , with the difference being more prominent near the zone center. The observation of more intense spin excitations in $\text{NaFe}_{0.53}\text{Cu}_{0.47}\text{As}$ is consistent with its larger ordered magnetic moment [25]. Intensities of spin excitations increase with the increase of momentum transfer, which is a result of RIXS probing the Brillouin zone centered around $(0, 0)$. This is distinct from INS measurements, which probe the Brillouin zones near $\mathbf{Q}_{\text{AF}} = (1, 0)$ or $(0, 1)$, where intensities of spin excita-

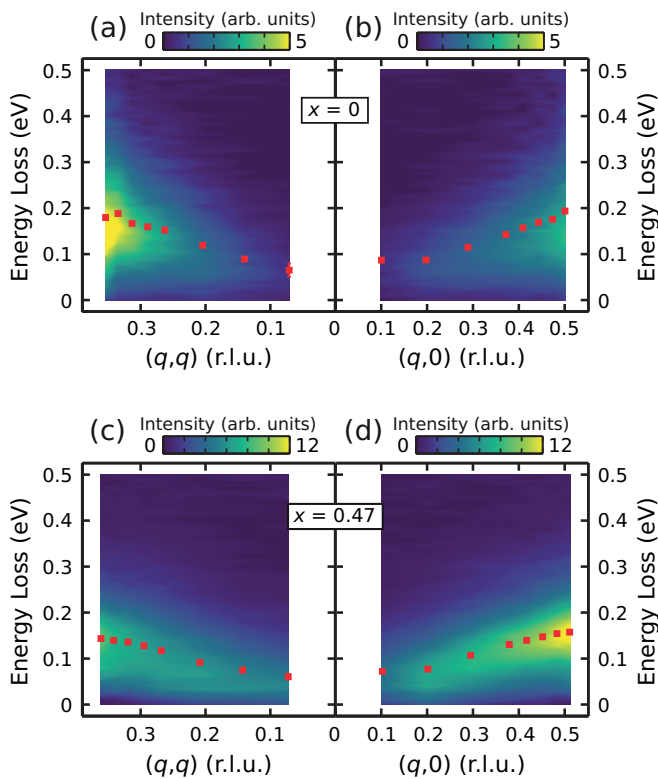


Figure 4: (Color online) Color-coded and interpolated intensities of spin excitations for NaFeAs along (a) (q, q) and (b) $(q, 0)$, and for NaFe_{0.53}Cu_{0.47}As along (c) (q, q) and (d) $(q, 0)$. Red symbols are E_0 extracted from our fitting. The intensities of spin excitations are obtained from our data, after subtracting fits to I_{fluor} , I_{bkg} and the elastic peak (as done for data in Fig. 8).

tions typically decrease when moving away from \mathbf{Q}_{AF} [42]. Moreover, Fig. 4 suggests that spin excitations in both NaFeAs and NaFe_{0.53}Cu_{0.47}As are dispersive, confirmed by energies of E_0 extracted from our fits (red symbols).

To further quantitatively compare the spin excitations in the two studied samples, fit results of E_0 and $\gamma/2$ are summarized in Figs. 5(a)-(b), as a function of the in-plane momentum transfer \mathbf{Q}_{ab} . As can be seen in Fig. 5(a), spin excitations in NaFeAs are systematically more energetic compared to those in NaFe_{0.53}Cu_{0.47}As. While the dispersions are almost isotropic for NaFeAs along the (q, q) and $(q, 0)$ directions, in NaFe_{0.53}Cu_{0.47}As the dispersion along $(q, 0)$ is clearly more energetic compared to (q, q) . $\gamma/2$, which parametrizes damping, is compared in Fig. 5(b). While similar damping rates are obtained for $|\mathbf{Q}_{ab}| \lesssim 0.3 \text{ \AA}^{-1}$, spin excitations in the $x = 0.47$ sample become clearly less damped compared to those in NaFeAs for $|\mathbf{Q}_{ab}| \gtrsim 0.3 \text{ \AA}^{-1}$. E_0 and $\gamma/2$ in Figs. 5(a) and (b) are plotted against the same vertical axis, which allows a direct comparison of the two quantities. This is important as spin excitations with a well-defined propagating energy can be assigned only when $\gamma/2 < E_0$

(underdamped), since when $\gamma/2 > E_0$ the spin excitations become overdamped and are non-propagating [59]. As can be seen in Figs. 5(a)-(b), $\gamma/2 < E_0$ is satisfied for all measurements in both $x = 0$ and $x = 0.47$ samples (within fit uncertainties). Our results suggest that although significant damping is present in both samples, the spin excitations remain underdamped, and can be described as spin waves associated with their respective magnetically-ordered ground states.

Given that Fe and Cu atoms order into chains in the ideal NaFe_{0.5}Cu_{0.5}As structure (Fig. 1(b)) [25], spin excitations in our $x = 0.47$ sample should be quasi-1D. The dispersion of spin waves in a 1D antiferromagnetically-ordered spin chain, with two spins in the unit cell along the chain direction (the K -direction in reciprocal space), is described within classical linear spin wave theory by:

$$E(\mathbf{Q}) = 2SJ \sin(K\pi), \quad (5)$$

with J being the nearest-neighbor exchange coupling and S being the size of the effective spin. For a quasi-1D system, long-range order is only possible when there are exchange interactions between the chains, which will add H and L dependencies to $E(\mathbf{Q})$. Nonetheless, it is reasonable to assume that J is the dominant interaction and spin waves probed in the energy scale of RIXS are mostly determined by J . Given that the (q, q) direction is unaffected by twinning, we fit its dispersion using the 1D model and obtained $SJ = 79.4(6) \text{ meV}$ (Fig. 6(a)). This value of SJ is then used to obtain the dispersion along the Fe chain direction (the $(0, K)$ direction, solid line in Fig. 6(b)), in comparison with our measurements along the $(q, 0)$ direction (symbols in Fig. 6(b)). As can be seen, the measured dispersion appears significantly lower in energy, which results from twinning. This is because the $(H, 0)$ direction is perpendicular to the Fe chains and exhibits spin excitations at considerably lower energies compared to the $(0, K)$ direction, and since our $(q, 0)$ measurements contain contributions from both $(H, 0)$ and $(0, K)$ directions, the measured energies along $(q, 0)$ are lower compared to what's expected for $(0, K)$. We note that due to strong quantum fluctuations in 1D, while the dispersion of spin excitation is well-described by Eq. 5, the factor 2 is replaced by π for $S = 1/2$ [64] and ≈ 2.8 for $S = 1$ [65]. This means that the extracted values of J based on classical linear spin wave theory could be overestimated by $\approx 57\%$ for $S = 1/2$ and $\approx 40\%$ for $S = 1$. In contrast, a much smaller overestimation is expected in two dimensions ($\approx 18\%$ for $S = 1/2$ on a square lattice [66]).

While spinons dominate the excitation spectrum of an ideal $S = 1/2$ antiferromagnetic spin chain, spin waves dominate the magnetically-ordered phase induced by inter-chain interactions [67]. The contribution from spinons also becomes less important for $S > 1/2$, and if spinons are present in NaFe_{0.53}Cu_{0.47}As, it would be challenging to distinguish them from the fluorescence. For the points closest to the zone center $\mathbf{Q}_{ab} = (0, 0)$ in Figs. 6(a) and (b), the data appears to deviate from

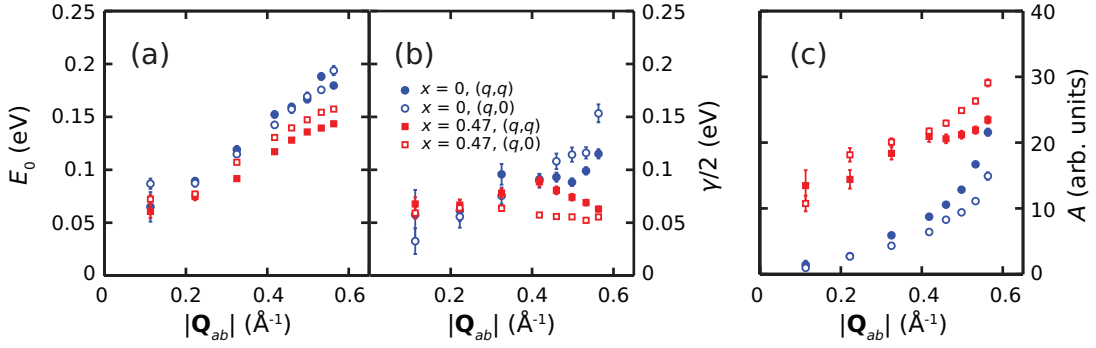


Figure 5: (Color online) Fit results of (a) E_0 , (b) $\gamma/2$ and (c) A , compared for NaFeAs and NaFe_{0.53}Cu_{0.47}As.

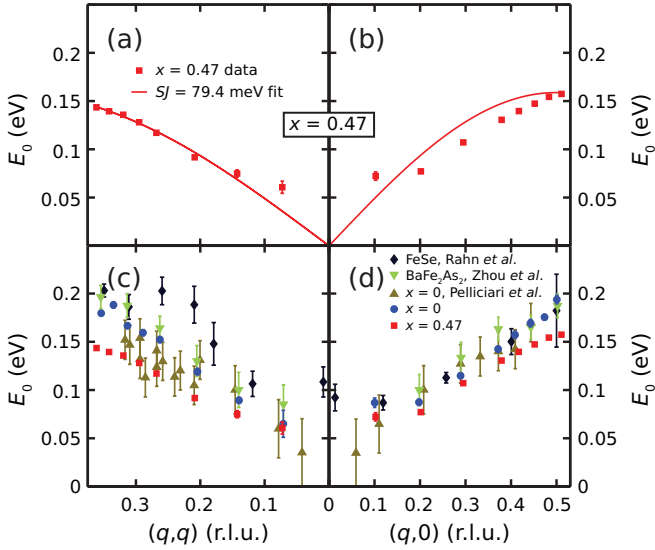


Figure 6: (Color online) (a) Fit to a classical 1D spin chain model, for the dispersion of spin excitations in NaFe_{0.53}Cu_{0.47}As along (q, q) , resulting in $SJ \approx 80$ meV. (b) Comparison of expected dispersion along $(0, K)$ (along the Fe chains) in NaFe_{0.53}Cu_{0.47}As ($SJ = 79.4$ meV) with the measured dispersion along $(q, 0)$. Comparisons of the dispersion of spin excitations from our measurements with previous results on BaFe₂As₂ [46], NaFeAs [49] and FeSe [53], along (c) (q, q) and (d) $(q, 0)$.

Eq. 5. This may suggest the presence of a sizable zone-center spin gap, or it may result from an overestimate of E_0 when its intrinsic value is small (as discussed in Section II. B.). INS measurements which probe spin excitations at the $(1,0)/(0,1)$ zone center would be able to distinguish these two scenarios.

We compare our RIXS results on NaFe_{1-x}Cu_xAs ($x = 0$ and $x = 0.47$) with previous results on BaFe₂As₂ [46], NaFeAs [49] and FeSe [53] in Figs. 6(c)-(d). We find our results on NaFeAs to be consistent with previous measurements [49], within experimental uncertainties. Along the (q, q) direction, spin excitations in FeSe are the most energetic, followed by those in BaFe₂As₂, NaFeAs and NaFe_{0.53}Cu_{0.47}As (Fig. 6(c)). Less contrast in the en-

ergy of spin excitations is observed along the $(q, 0)$ direction, with NaFe_{0.53}Cu_{0.47}As being slightly less energetic than the other compounds (Fig. 6(d)).

Starting from NaFeAs and doping Co to span the phase diagram encompassing the superconducting dome, it was shown that high-energy ($\gtrsim 20$ meV) spin excitations exhibit little variation with doping [49, 68]. As similar observations were also made for BaFe_{2-x}Ni₂As₂ [69], such a behavior should be general for electron-doped FeSCs. Since Cu dopes electrons near the superconducting dome [70, 71], we expect high-energy spin excitations in superconducting NaFe_{1-x}Cu_xAs to be similar to those in NaFeAs. This means that the softening we observe in NaFe_{0.53}Cu_{0.47}As likely occurs when doping well beyond the superconducting dome.

IV. DISCUSSION AND CONCLUSION

As Cu was shown to have +1 valence and to be non-magnetic in NaFe_{1-x}Cu_xAs when $x \approx 0.5$ (see Supplementary Information of Ref. [25]), valence counting suggests Fe ions to have a 3+ valence and correspond to a $n = 5$ state. The present findings instead indicate Fe ions having a 2+ valence and remains in a $n = 6$ state upon Cu-doping, similar to NaFeAs. This is consistent with the similar local atomic environment found in the two cases (Fig. 1(c)-(d)), and suggests that As ions have an unusual -2.5 valence. Therefore, even though As-As covalent bonding along the c -axis as in BaCu₂As₂ [39] is not possible, a change of As nominal valence in NaFe_{1-x}Cu_xAs occurs upon Cu-substitution ($\text{As}^{3-} \rightarrow \text{As}^{2.5-}$), and is associated with a reduction of the c -axis lattice parameter ($c = 6.97 \text{ \AA} \rightarrow c = 6.88 \text{ \AA}$). It appears that the holes contributed through Cu-doping reside on the As sites, rather than the Fe sites. This is analogous to the hole-doped cuprates, in which the doped holes reside on the O sites rather than the Cu sites. This charge transfer physics deserves further theoretical and experimental investigations.

The nearest-neighbor exchange coupling $SJ \approx 80$ meV obtained within classical linear spin wave theory for NaFe_{0.53}Cu_{0.47}As can be compared against effective ex-

change couplings obtained for the parent compounds of FeSCs. A comparison between the magnetic structures of NaFeAs and NaFe_{0.5}Cu_{0.5}As (Figs. 1(a)-(b)) shows that the latter can be obtained by replacing half of the Fe ions in NaFeAs by nonmagnetic Cu ions (and an in-plane 90°-rotation of spins), thus there is a correspondence between SJ_{1a} in NaFeAs and SJ in NaFe_{0.5}Cu_{0.5}As. SJ_{1a} for archetypal parent compounds of FeSCs are ≈ 40 meV for NaFeAs [44], ≈ 59 meV for BaFe₂As₂ [72], ≈ 50 meV for CaFe₂As₂ [73] and $\approx 31 - 39$ meV for SrFe₂As₂ [74]. SJ in our $x = 0.47$ sample is clearly larger than SJ_{1a} in parent compounds of the FeSCs (the larger bandwidths of spin excitations in the latter include contributions from SJ_{1b} and SJ_2), within classical linear spin wave theory. The larger value of SJ in NaFe_{0.53}Cu_{0.47}As could be the result of a larger exchange coupling J , a larger S or stronger quantum fluctuations (which leads to a larger overestimation of SJ within classical linear spin wave theory). To differentiate between these possibilities, it would be desirable to map out magnetic excitations over the Brillouin zone using inelastic neutron scattering, which allows S and J to be independently determined [42]. Once S is determined, the overestimation of J due to quantum fluctuations can also be corrected for.

Density functional theory (DFT) [25, 29] and DFT+dynamical mean field theory (DMFT) calculations [27] suggest NaFe_{0.5}Cu_{0.5}As to be metallic in the paramagnetic state, while experimentally semiconducting/insulating transport persists above $T_N \approx 200$ K. This difference may result from strong electronic correlations not fully captured by DFT and DFT+DMFT calculations [25, 29], which results in NaFe_{0.5}Cu_{0.5}As being a Mott insulator. Alternatively, it has been suggested that short-range spin correlations persist above T_N , and NaFe_{0.5}Cu_{0.5}As is a Slater insulator. Our finding of $SJ \approx 80$ meV suggests the dominant exchange interaction energy is substantially larger than $k_B T_N$, and implies the presence of spin fluctuations above T_N . Ideally, to differentiate whether NaFe_{0.5}Cu_{0.5}As is a Mott insulator or a Slater insulator, its transport properties for $k_B T \gg J$ should be studied; however, since $k_B J$ is comparable to the melting temperature of NaFe_{0.5}Cu_{0.5}As, this is difficult to achieve experimentally.

To shed light on the nature of the insulating state of NaFe_{0.5}Cu_{0.5}As, we calculated the theoretical phase diagram of NaFe_{0.5}Cu_{0.5}As using $U(1)$ slave-spin mean field theory (with Fe ions in the $n = 6$ state), with results shown in Fig. 7. Consistent with previous studies of multiorbital models [12, 13], we find that for $n = 6$ the Mott insulating state survives in a significantly smaller parameter space, compared to half-filling ($n = 5$). Using the band renormalization factor obtained from ARPES measurements for NaFeAs [75], we estimated the physical regime of U and J_H for NaFeAs [25]. Given the similar local environment and valence of Fe ions in NaFeAs and NaFe_{0.5}Cu_{0.5}As, this regime of U and J_H is then extended to the latter compound. As can be seen, while the

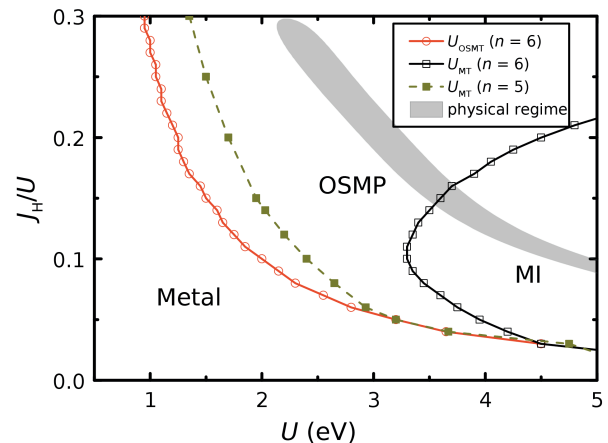


Figure 7: Theoretical phase diagram of NaFe_{0.5}Cu_{0.5}As. The shaded gray area is the expected physical regime that the system resides in. Depending on the values of Hubbard repulsion U and Hund's coupling J_H , the system may be a metal, an orbitally-selective Mott phase (OSMP), or a Mott insulator (MI). For a fixed J_H/U , the system may experience an orbitally-selective Mott transition ($U = U_{OSMT}$) and a Mott transition ($U = U_{MT}$), with the increase of U . The line of U_{OSMT} for $n = 5$ is similar to that of $n = 6$ [25].

physical regime is entirely inside the Mott insulator state of $n = 5$, it is only partially inside the Mott insulating state of $n = 6$.

Our theoretical results suggest that depending on the precise values of U and J_H , NaFe_{0.5}Cu_{0.5}As may either be in a Mott insulating state or a orbital-selective Mott insulating state, with the Slater mechanism relevant for the insulating transport behavior in the latter case. It should be emphasized that in both scenarios, strong electronic correlations are essential for the insulating behavior in NaFe_{0.5}Cu_{0.5}As. Near the boundary that separates the two cases, we expect a crossover in Mott-type and Slater-type behavior, where distinctions between the two are blurred. NaFe_{0.5}Cu_{0.5}As is thus a rare example of a $n = 6$ multiorbital correlated insulator continuously connected to unconventional superconductivity, similar to BaFe₂S₃ and BaFe₂Se₃ [15, 17, 18]. In the latter compounds, the semiconducting/insulating behavior under ambient pressure was attributed to Mott physics [16, 76–78] or a Slater mechanism [79]. It is interesting to note the RIXS spectra of BaFe₂Se₃ are dominated by dd -excitations, which are typically strongly suppressed in the iron pnictides [47], this suggests larger U in BaFe₂Se₃ compared to the iron pnictides. Similar crossover between Mott-type and Slater-type insulating behavior has been discussed for the iridates Sr₂IrO₄ [80–82] and Nd₂Ir₂O₇ [83].

As demonstrated using other techniques [84], it should be possible to detwin NaFeAs (or other parent compounds of FeSCs) by applying a small strain in RIXS experiments. For NaFe_{0.53}Cu_{0.47}As, as twinning is due to Fe-Cu ordering already present at room temperature, it is unlikely strain will have a similar detwin-

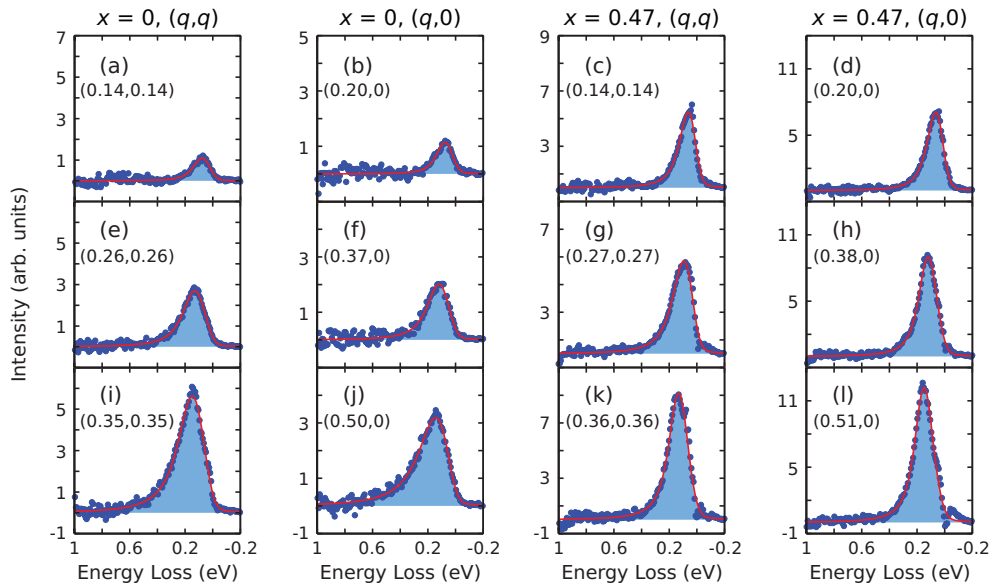


Figure 8: Similar scans as in Fig. 3, but showing only I_{spin} (red lines and light blue shaded areas). Fit values of I_{bkg} , I_{fluo} and the elastic peak have been subtracted from the measured data (blue symbols).

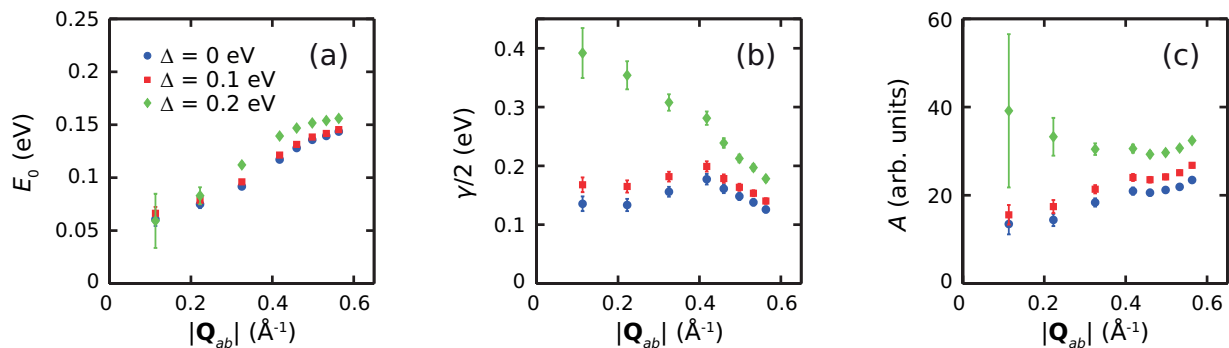


Figure 9: Comparison of fit results for the fit parameters (a) E_0 , (b) $\gamma/2$, and (c) A , with the introduction of a gap Δ in I_{fluo} (Eq. 3). The fits are for data on $\text{NaFe}_{0.53}\text{Cu}_{0.47}\text{As}$ along (q, q) .

ning effect. Nonetheless, it is conceivable that Fe-Cu ordering may disappear at a higher temperature. Applying strain above such a temperature and cooling to room temperature could lead to a detwinned sample. It may be desirable to pursue such a strategy in heavily-doped $\text{NaFe}_{1-x}\text{Cu}_x\text{As}$ to reveal the system's in-plane anisotropic physical properties using RIXS and other experimental probes.

In conclusion, we show that Fe ions in $\text{NaFe}_{1-x}\text{Cu}_x\text{As}$ remains in a $n = 6$ state for both $x = 0$ and $x = 0.47$. RIXS measurements demonstrate the presence of underdamped dispersive spin excitations in both cases. Compared to NaFeAs , spin excitations in $\text{NaFe}_{0.53}\text{Cu}_{0.47}\text{As}$ are slightly softened in energy but significantly enhanced in intensity. In addition, the dispersion of spin excitations is consistent with arising from localized quasi-one-dimensional magnetic moments. Our results suggest that $\text{NaFe}_{0.5}\text{Cu}_{0.5}\text{As}$ likely resides in a crossover regime between Mott-type and Slater-type insulating behavior,

and strong electronic correlations are essential for realizing its insulating state.

V. ACKNOWLEDGMENTS

The RIXS work at Rice is supported by the US Department of Energy (DOE), Basic Energy Sciences (BES), under Contract No. DE-SC0012311 (P.D.). The materials synthesis efforts at Rice are supported by the Robert A. Welch Foundation, Grant No. C-1839 (P.D.). The work at the University of California, Berkeley and Lawrence Berkeley National Laboratory was supported by the Office of Science, Office of Basic Energy Sciences, Materials Sciences and Engineering Division, of the U.S. Department of Energy (DOE) under Contract No. DE-AC02-05-CH11231 within the Quantum Materials Program (KC2202). J.P. and T.S. acknowledge financial support through the Dysenos AG by Kabelwerke Brugg

AG Holding, Fachhochschule Nordwestschweiz, and the Paul Scherrer Institut. The synchrotron radiation experiments have been performed at the ADDRESS beamline of the Swiss Light Source at the Paul Scherrer Institut. Part of this research has been funded by the Swiss National Science Foundation through the D-A-CH program (SNSF Research Grant No. 200021L 141325). The work at PSI is supported by the Swiss National Science Foundation through the NCCR MARVEL and the Sinergia network Mott Physics Beyond the Heisenberg Model (MPBH) (SNSF Research Grants No. CRSII2_160765/1 and No. CRSII2_141962). X.L. acknowledges financial support from the European Community's Seventh Framework Program (FP7/2007-2013) under Grant Agreement No. 290605 (COFUND: PSI-FELLOW).

VI. APPENDIX

A. Comparison between data and fit spin excitations

To allow a direct comparison between our data and fit spin excitations, fits to I_{flu} , I_{bkg} and the elastic peak are

subtracted from Fig. 3 and shown in Fig. 8. This allows the fit I_{spin} to be directly compared with experimental data. As can be seen, good fits to the model of I_{spin} have been achieved in all cases.

B. Effect of a gap in the fluorescence on fit results

Since $\text{NaFe}_{1-x}\text{Cu}_x\text{As}$ with $x \approx 0.5$ is a semiconductor with a lowest electronic gap ≈ 0.1 eV [27], we considered modeling its fluorescence using a gapped form (Eq. 3), which reduces to Eq. 2 when the gap Δ becomes 0. All of our analysis in the main text were fit using Eq. 2 for I_{flu} . In Fig. 9, we compare fit results of E_0 , $\gamma/2$ and A with $\Delta = 0, 0.1$ and 0.2 eV, for $\text{NaFe}_{0.53}\text{Cu}_{0.47}\text{As}$ along (q, q) . With the increase of Δ , the fit values of E_0 , $\gamma/2$ and A all increases, with the change being rather small for $\Delta = 0.1$ eV. Similar results are also obtained for data along $(q, 0)$.

This analysis suggests that the experimentally obtained charge gap ≈ 0.1 eV is unlikely to significantly affect our fit results. Moreover, our conclusion of enhanced magnetic fluctuations in $\text{NaFe}_{0.53}\text{Cu}_{0.47}\text{As}$ compared to NaFeAs remains robust with the increase of Δ .

-
- [1] Patrick A. Lee, Naoto Nagaosa, and Xiao-Gang Wen, *Doping a Mott insulator: Physics of high-temperature superconductivity*, Rev. Mod. Phys. **78**, 17 (2006).
- [2] D. J. Scalapino, Rev. Mod. Phys. **84**, 1383 (2012).
- [3] R. Coldea, S.M. Hayden, G. Aeppli, T.G. Perring, C.D. Frost, T.E. Mason, S.-W. Cheong, Z. Fisk, *Spin waves and electronic interactions in La_2CuO_4* , Phys. Rev. Lett. **86**, 5377 (2001).
- [4] Robert J. Birgeneau, Chris Stock, John M. Tranquada, and Kazuyoshi Yamada, *Magnetic Neutron Scattering in Hole-Doped Cuprate Superconductors*, J. Phys. Soc. Jpn. **75**, 111003 (2006).
- [5] Yvan Sidis, Stéphane Pailhès, Vladimir Hinkov, Benoît Fauqué, Clemens Ulrich, Lucia Capogna, Alexandre Ivanov, Louis-Pierre Regnault, Bernhard Keimer, Philippe Bourges, *Inelastic neutron scattering study of spin excitations in the superconducting state of high temperature superconductors*, C. R. Phys. **8**, 745 (2007).
- [6] Masaki Fujita, Haruhiro Hiraka, Masaaki Matsuda, Masato Matsuura, John M. Tranquada, Shuichi Wakimoto, Guangyong Xu, and Kazuyoshi Yamada, *Progress in Neutron Scattering Studies of Spin Excitations in High- T_c Cuprates*, J. Phys. Soc. Jpn. **81**, 011007 (2012).
- [7] M. P. M. Dean, *Insights into the high temperature superconducting cuprates from resonant inelastic X-ray scattering*, J. Magn. Magn. Mater. **376**, 3-13 (2015).
- [8] M. M. Qazilbash, J. J. Hamlin, R. E. Baumbach, Lijun Zhang, D. J. Singh, M. B. Maple and D. N. Basov, *Electronic correlations in the iron pnictides*, Nat. Phys. **5**, 647-650 (2009).
- [9] Z. P. Yin, K. Haule and G. Kotliar, *Kinetic frustration and the nature of the magnetic and paramagnetic states in iron pnictides and iron chalcogenides*, Nat. Mater. **10**, 932-935 (2011).
- [10] Pengcheng Dai, Jiangping Hu and Elbio Dagotto, *Magnetism and its microscopic origin in iron-based high-temperature superconductors*, Nat. Phys. **8**, 709-718 (2012).
- [11] Qimiao Si, Rong Yu and Elihu Abrahams, *High-temperature superconductivity in iron pnictides and chalcogenides*, Nat. Rev. Mater. **1**, 16017 (2016).
- [12] Luca de' Medici, Jernej Mravlje, and Antoine Georges, *Janus-Faced Influence of Hund's Rule Coupling in Strongly Correlated Materials*, Phys. Rev. Lett. **107**, 256401 (2011).
- [13] L. Fanfarillo and E. Bascones, *Electronic correlations in Hund metals*, Phys. Rev. B **92**, 075136 (2015).
- [14] Qimiao Si and Elihu Abrahams, *Strong Correlations and Magnetic Frustration in the High T_c Iron Pnictides*, Phys. Rev. Lett. **101**, 076401 (2008).
- [15] Hiroki Takahashi, Akira Sugimoto, Yusuke Nambu, Touru Yamauchi, Yasuyuki Hirata, Takateru Kawakami, Maxim Avdeev, Kazuyuki Matsubayashi, Fei Du, Chizuru Kawashima, Hideto Soeda, Satoshi Nakano, Yoshiya Uwatoko, Yutaka Ueda, Taku J. Sato and Kenya Ohgushi, *Pressure-induced superconductivity in the iron-based ladder material BaFe_2S_3* , Nat. Mater. **14**, 1008-1012 (2015).
- [16] Touru Yamauchi, Yasuyuki Hirata, Yutaka Ueda, and Kenya Ohgushi, *Pressure-Induced Mott Transition Followed by a 24-K Superconducting Phase in BaFe_2S_3* , Phys. Rev. Lett. **115**, 246402 (2015).
- [17] Jianjun Ying, Hechang Lei, Cedomir Petrovic, Yuming Xiao, and Viktor V. Struzhkin, *Interplay of magnetism and superconductivity in the compressed Fe-ladder compound BaFe_2Se_3* , Phys. Rev. B **95**, 241109(R) (2017).

- [18] Songxue Chi, Yoshiya Uwatoko, Huibo Cao, Yasuyuki Hirata, Kazuki Hashizume, Takuya Aoyama, and Kenya Ohgushi, *Magnetic Precursor of the Pressure-Induced Superconductivity in Fe-Ladder Compounds*, Phys. Rev. Lett. **117**, 047003 (2016).
- [19] Luca de' Medici, Gianluca Giovannetti, and Massimo Capone, *Selective Mott Physics as a Key to Iron Superconductors*, Phys. Rev. Lett. **112**, 177001 (2014).
- [20] Dinah R. Parker, Michael J. Pitcher, Peter J. Baker, Isabel Franke, Tom Lancaster, Stephen J. Blundell and Simon J. Clarke, *Structure, antiferromagnetism and superconductivity of the layered iron arsenide NaFeAs*, Chem. Commun. **16**, 2189-2191 (2009).
- [21] S. L. Li, C. de la Cruz, Q. Huang, G. F. Chen, T.-L. Xia, J. L. Luo, N. L. Wang, and P. C. Dai, *Structural and magnetic phase transitions in Na_{1- δ} FeAs*, Phys. Rev. B **80**, 020504 (2009).
- [22] J. D. Wright, T. Lancaster, I. Franke, A. J. Steele, J. S. Möller, M. J. Pitcher, A. J. Corkett, D. R. Parker, D. G. Free, F. L. Pratt, P. J. Baker, S. J. Clarke, and S. J. Blundell, *Gradual destruction of magnetism in the superconducting family NaFe_{1-x}Co_xAs*, Phys. Rev. B **85**, 054503 (2012).
- [23] A. F. Wang, J. J. Lin, P. Cheng, G. J. Ye, F. Chen, J. Q. Ma, X. F. Lu, B. Lei, X. G. Luo, and X. H. Chen, *Phase diagram and physical properties of NaFe_{1-x}Cu_xAs single crystals*, Phys. Rev. B **88**, 094516 (2013).
- [24] Cun Ye, Wei Ruan, Peng Cai, Xintong Li, Aifeng Wang, Xianhui Chen, and Yayu Wang, *Strong Similarities between the Local Electronic Structure of Insulating Iron Pnictide and Lightly Doped Cuprate*, Phys. Rev. X **5**, 021013 (2015).
- [25] Yu Song, Zahra Yamani, Chongde Cao, Yu Li, Chenglin Zhang, Justin S. Chen, Qingzhen Huang, Hui Wu, Jing Tao, Yimei Zhu, Wei Tian, Songxue Chi, Huibo Cao, Yao-Bo Huang, Marcus Dantz, Thorsten Schmitt, Rong Yu, Andriy H. Nevidomskyy, Emilia Morosan, Qimiao Si, and Pengcheng Dai, *A Mott insulator continuously connected to iron pnictide superconductors*, Nat. Commun. **7**, 13879 (2016). <https://doi.org/10.1038/ncomms13879>
- [26] C. E. Matt, N. Xu, Baiqing Lv, Junzhang Ma, F. Bisti, J. Park, T. Shang, Chongde Cao, Yu Song, Andriy H. Nevidomskyy, Pengcheng Dai, L. Patthey, N. C. Plumb, M. Radovic, J. Mesot, and M. Shi, *NaFe_{0.56}Cu_{0.44}As: A Pnictide Insulating Phase Induced by OnSite Coulomb Interaction*, Phys. Rev. Lett. **117**, 097001 (2016).
- [27] A. Charnukha, Z. P. Yin, Y. Song, C. D. Cao, Pengcheng Dai, K. Haule, G. Kotliar, and D. N. Basov, *Correlation-driven metal-insulator transition in proximity to an iron-based superconductor*, Phys. Rev. B **96**, 195121 (2017).
- [28] Yizhou Xin, Ingrid Stolt, Yu Song, Pengcheng Dai, and W. P. Halperin, *Stripe antiferromagnetism and disorder in the Mott insulator NaFe_{1-x}Cu_xAs ($x \lesssim 0.5$)*, Phys. Rev. B **101**, 064410 (2020).
- [29] Shunhong Zhang, Yanjun He, Jia-Wei Mei, Feng Liu, and Zheng Liu, *Electronic and spin dynamics in the insulating iron pnictide NaFe_{0.5}Cu_{0.5}As*, Phys. Rev. B **96**, 245128 (2017).
- [30] S. L. Skornyakov, V. I. Anisimov, and I. Leonov, *Orbital-selective coherence-incoherence crossover and metal-insulator transition in Cu-doped NaFeAs*, arXiv:2101.03776 (2021).
- [31] A. A. Vaipolin, S. A. Kijaev, L. V. Kradinova, A. M. Polubotko, V. V. Popov, V. D. Prochukhan, Y. V. Rud, and V. E. Skoriukin, *Investigation of the gapless state in CuFeTe₂*, J. Phys. Condens. Matter **4**, 8035 (1992).
- [32] F. N. Abdullaev, T. G. Kerimova, G. D. Sultanov, and N. A. Abdullaev, *Conductivity Anisotropy and Localization of Charge Carriers in CuFeTe₂ Single Crystals with a Layered Structure*, Phys. Solid State **48**, 1848 (2006).
- [33] D. A. Zocco, D. Y. Tütün, J. J. Hamlin, J. R. Jeffries, S. T. Weir, Y. K. Vohra, and M. B. Maple, *High pressure transport studies of the LiFeAs analogs CuFeTe₂ and Fe₂As*, Supercond. Sci. Technol. **25**, 084018 (2012).
- [34] Patrick N. Valdivia, Min Gyu Kim, Thomas R. Forrest, Zhijun Xu, Meng Wang, Hui Wu, Leland W. Harringer, Edith D. Bourret-Courchesne, and Robert J. Birgeneau, *Copper-substituted iron telluride: A phase diagram*, Phys. Rev. B **91**, 224424 (2015).
- [35] Y. J. Yan, P. Cheng, J. J. Ying, X. G. Luo, F. Chen, H. Y. Zou, A. F. Wang, G. J. Ye, Z. J. Xiang, J. Q. Ma, and X. H. Chen, *Structural, magnetic, and electronic transport properties of hole-doped SrFe_{2-x}Cu_xAs₂ single crystals*, Phys. Rev. B **87**, 075105 (2013).
- [36] Weiyi Wang, Yu Song, Ding Hu, Yu Li, Rui Zhang, L. W. Harringer, Wei Tian, Huibo Cao, and Pengcheng Dai, *Local breaking of fourfold rotational symmetry by short-range magnetic order in heavily overdoped Ba(Fe_{1-x}Cu_x)₂As₂*, Phys. Rev. B **96**, 161106(R) (2017).
- [37] Ming Yi, Yan Zhang, Zhi-Xun Shen and Donghui Lu, *Role of the orbital degree of freedom in iron-based superconductors*, npj Quant. Mater. **2**, 57 (2017).
- [38] A. Kreyssig, M. A. Green, Y. Lee, G. D. Samolyuk, P. Zajdel, J. W. Lynn, S. L. Bud'ko, M. S. Torikachvili, N. Ni, S. Nandi, J. B. Leão, S. J. Poulton, D. N. Argyriou, B. N. Harmon, R. J. McQueeney, P. C. Canfield, and A. I. Goldman, *Pressure-induced volume-collapsed tetragonal phase of CaFe₂As₂ seen via neutron scattering*, Phys. Rev. B **78**, 184517 (2008).
- [39] V. K. Anand, P. Kanchana Perera, Abhishek Pandey, R. J. Goetsch, A. Kreyssig, and D. C. Johnston, *Crystal growth and physical properties of SrCu₂As₂, SrCu₂Sb₂, and BaCu₂Sb₂*, Phys. Rev. B **85**, 214523 (2012).
- [40] N. Mannella, *The magnetic moment enigma in Fe-based high temperature superconductors*, J. Phys.: Condens. Matter **26**, 473202 (2014).
- [41] C. Watzenbock, M. Edelmann, D. Springer, G. Sangiovanni, and A. Toschi, *Characteristic Timescales of the Local Moment Dynamics in Hund's Metals*, Phys. Rev. Lett. **125**, 086402 (2020).
- [42] Pengcheng Dai, *Antiferromagnetic order and spin dynamics in iron-based superconductors*, Rev. Mod. Phys. **87**, 855 (2015).
- [43] Dmytro S. Inosov, *Spin fluctuations in iron pnictides and chalcogenides: From antiferromagnetism to superconductivity*, C. R. Physique **17**, 60-89 (2016).
- [44] Chenglin Zhang, Leland W. Harringer, Zhiping Yin, Weicheng Lv, Miaoyin Wang, Guotai Tan, Yu Song, D. L. Abernathy, Wei Tian, Takeshi Egami, Kristjan Haule, Gabriel Kotliar, and Pengcheng Dai, *Effect of Pnictogen Height on Spin Waves in Iron Pnictides*, Phys. Rev. Lett. **112**, 217202 (2014).
- [45] Luuk J. P. Ament, Michel van Veenendaal, Thomas P. Devereaux, John P. Hill, and Jeroen van den Brink, *Res-*

- onant inelastic x-ray scattering studies of elementary excitations, *Rev. Mod. Phys.* **83**, 705 (2011).
- [46] Ke-Jin Zhou, Yao-Bo Huang, Claude Monney, Xi Dai, Vladimir N. Strocov, Nan-Lin Wang, Zhi-Guo Chen, Chenglin Zhang, Pengcheng Dai, Luc Patthey, Jeroen van den Brink, Hong Ding, and Thorsten Schmitt, *Persistent high-energy spin excitations in iron-pnictide superconductors*, *Nat. Commun.* **4**, 1470 (2013).
- [47] C. Monney, A. Uldry, K. J. Zhou, A. Krzton-Maziopa, E. Pomjakushina, V. N. Strocov, B. Delley, and T. Schmitt, *Resonant inelastic x-ray scattering at the Fe L_3 edge of the one-dimensional chalcogenide $BaFe_2Se_3$* , *Phys. Rev. B* **88**, 165103 (2013).
- [48] H. Gretarsson, T. Nomura, I. Jarrige, A. Lupascu, M. H. Upton, Jungho Kim, D. Casa, T. Gog, R. H. Yuan, Z. G. Chen, N.-L. Wang, and Young-June Kim, *Resonant inelastic x-ray scattering study of electronic excitations in insulating $Ko_{0.83}Fe_{1.53}Se_2$* , *Phys. Rev. B* **91**, 245118 (2015).
- [49] Jonathan Pelliciari, Yaobo Huang, Tanmoy Das, Marcus Dantz, Valentina Bisogni, Paul Olalde Velasco, Vladimir N. Strocov, Lingyi Xing, Xiancheng Wang, Changqing Jin, and Thorsten Schmitt, *Intralayer doping effects on the high-energy magnetic correlations in $NaFeAs$* , *Phys. Rev. B* **93**, 134515 (2016).
- [50] T. Nomura, Y. Harada, H. Niwa, K. Ishii, M. Ishikado, S. Shamoto, and I. Jarrige, *Resonant inelastic x-ray scattering study of entangled spin-orbital excitations in superconducting $PrFeAsO_{0.7}$* , *Phys. Rev. B* **94**, 035134 (2016).
- [51] Jonathan Pelliciari, Marcus Dantz, Yaobo Huang, Vladimir N. Strocov, Lingyi Xing, Xiancheng Wang, Changqing Jin, and Thorsten Schmitt, *Presence of magnetic excitations in $SmFeAsO$* , *Appl. Phys. Lett.* **109**, 122601 (2016).
- [52] Jonathan Pelliciari, Kenji Ishii, Marcus Dantz, Xingye Lu, Daniel E. McNally, Vladimir N. Strocov, Lingyi Xing, Xiancheng Wang, Changqing Jin, Hirale S. Jeevan, Philipp Gegenwart, and Thorsten Schmitt, *Local and collective magnetism of $EuFe_2As_2$* , *Phys. Rev. B* **95**, 115152 (2017).
- [53] M. C. Rahn, K. Kummer, N. B. Brookes, A. A. Haghighirad, K. Gilmore, and A. T. Boothroyd, *Paramagnon dispersion in β - $FeSe$ observed by Fe L -edge resonant inelastic x-ray scattering*, *Phys. Rev. B* **99**, 014505 (2019).
- [54] Fernando A. Garcia, Oleh Ivashko, Daniel E. McNally, Lakshmi Das, Mario M. Piva, C. Adriano, Pascoal G. Pagliuso, Johan Chang, Thorsten Schmitt, and Claude Monney, *Anisotropic magnetic excitations and incipient Néel order in $Ba(Fe_{1-x}Mn_x)_2As_2$* , *Phys. Rev. B* **99**, 115118 (2019).
- [55] Jonathan Pelliciari, Kenji Ishii, Yaobo Huang, Marcus Dantz, Xingye Lu, Paul Olalde-Velasco, Vladimir N. Strocov, Shigeru Kasahara, Lingyi Xing, Xiancheng Wang, Changqing Jin, Yuji Matsuda, Takasada Shibauchi, Tanmoy Das and Thorsten Schmitt, *Reciprocity between local moments and collectivemagnetic excitations in the phase diagram of $BaFe_2(As_{1-x}P_x)_2$* , *Commun. Phys.* **2**, 139 (2019).
- [56] V. N. Strocov, T. Schmitt, U. Flechsig, T. Schmidt, A. Imhof, Q. Chen, J. Raabe, R. Betemps, D. Zimoch, J. Krempasky, X. Wang, M. Grioni, A. Piazzalunga, and L. Patthey, *High-resolution soft X-ray beamline ADDRESS at the Swiss Light Source for resonant inelastic X-ray scattering and angle-resolved photoelectron spectroscopies*, *J. Synchrotron Radiat.* **17**, 631 (2010).
- [57] G. Ghiringhelli, A. Piazzalunga, C. Dallera, G. Trezzi, L. Braicovich, T. Schmitt, V. N. Strocov, R. Betemps, L. Patthey, X. Wang, and M. Grioni, *SAXES, a high resolution spectrometer for resonant x-ray emission in the 400–1600 eV energy range*, *Rev. Sci. Instrum.* **77**, 113108 (2006).
- [58] Yu Song, Louis-Pierre Regnault, Chenglin Zhang, Guotai Tan, Scott V. Carr, Songxue Chi, A. D. Christianson, Tao Xiang, and Pengcheng Dai, *In-plane spin excitation anisotropy in the paramagnetic state of $NaFeAs$* , *Phys. Rev. B* **88**, 134512 (2013).
- [59] Jagat Lamsal and Wouter Montfrooij, *Extracting paramagnon excitations from resonant inelastic x-ray scattering experiments*, *Phys. Rev. B* **93**, 214513 (2016).
- [60] Rong Yu and Qimiao Si, *$U(1)$ slave-spin theory and its application to Mott transition in a multiorbital model for iron pnictides*, *Phys. Rev. B* **86**, 085104 (2012).
- [61] Rong Yu, Jian-Xin Zhu, and Qimiao Si, *Orbital-selective superconductivity, gap anisotropy, and spin resonance excitations in a multiorbital t - J_1 - J_2 model for iron pnictides*, *Phys. Rev. B* **89**, 024509 (2014).
- [62] Hyun Woo Kim, D. H. Kim, Eunsook Lee, Seungho Seong, J.-S. Kang, Deok Hyeon Kim, B. W. Lee, Y. Ko, and J.-Y. Kim, *Soft X-ray absorption spectroscopy study of multiferroic Bi-substituted $Ba_{1-x}Bi_xTi_{0.9}Fe_{0.1}O_3$* , *J. Korean Phys. Soc.* **69**, 361-364 (2016).
- [63] *X-Ray Diffraction*, B. E. Warren (Addison-Wesley, Reading, MA, 1969).
- [64] Jacques des Cloizeaux and J. J. Pearson, *Spin-Wave Spectrum of the Antiferromagnetic Linear Chain*, *Phys. Rev.* **128** 2131 (1962).
- [65] Shaolong Ma, Collin Broholm, Daniel H. Reich, B. J. Sternlieb and R. W. Erwin, *Dominance of Long-Lived Excitations in the Antiferromagnetic Spin-1 Chain NENP*, *Phys. Rev. Lett.* **69**, 3571 (1992).
- [66] R. Coldea, S. M. Hayden, G. Aeppli, T. G. Perring, C. D. Frost, T. E. Mason, S.-W. Cheong, and Z. Fisk, *Spin Waves and Electronic Interactions in La_2CuO_4* , *Phys. Rev. Lett.* **86**, 5377 (2001).
- [67] Bella Lake, D. Alan Tennant, Chris D. Frost, and Stephen E. Nagler, *Quantum criticality and universal scaling of a quantum antiferromagnet*, *Nat. Mater.* **4**, 329-334 (2005).
- [68] Scott V. Carr, Chenglin Zhang, Yu Song, Guotai Tan, Yu Li, D. L. Abernathy, M. B. Stone, G. E. Granroth, T. G. Perring, and Pengcheng Dai, *Electron doping evolution of the magnetic excitations in $NaFe_{1-x}Co_xAs$* , *Phys. Rev. B* **93**, 214506 (2016).
- [69] Huiqian Luo, Xingye Lu, Rui Zhang, Meng Wang, E. A. Goremychkin, D. T. Adroja, Sergey Danilkin, Guochu Deng, Zahra Yamani, and Pengcheng Dai, *Electron doping evolution of the magnetic excitations in $BaFe_{2-x}Ni_xAs_2$* , *Phys. Rev. B* **88**, 144516 (2013).
- [70] S. T. Cui, S. Kong, S. L. Ju, P. Wu, A. F. Wang, X. G. Luo, X. H. Chen, G. B. Zhang, and Z. Sun, *ARPES study of the effect of Cu substitution on the electronic structure of $NaFeAs$* , *Phys. Rev. B* **88**, 245112 (2013).
- [71] Yang Liu, Da-Yong Liu, Jiang-Long Wang, Jian Sun, Yun Song, and Liang-Jian Zou, *Localization and orbital selec-*

- tivity in iron-based superconductors with Cu substitution, Phys. Rev. B **92**, 155146 (2015).
- [72] L. W. Harriger, H. Q. Luo, M. S. Liu, C. Frost, J. P. Hu, M. R. Norman, and Pengcheng Dai, *Nematic spin fluid in the tetragonal phase of BaFe₂As₂*, Phys. Rev. B **84**, 054544 (2011).
- [73] Jun Zhao, D. T. Adroja, Dao-Xin Yao, R. Bewley, Shiliang Li, X. F. Wang, G. Wu, X. H. Chen, Jiangping Hu, and Pengcheng Dai, *Spin waves and magnetic exchange interactions in CaFe₂As₂*, Nat. Phys. **5**, 555 (2009).
- [74] R. A. Ewings, T. G. Perring, J. Gillett, S. D. Das, S. E. Sebastian, A. E. Taylor, T. Guidi, and A. T. Boothroyd, *Itinerant spin excitations in SrFe₂As₂ measured by inelastic neutron scattering*, Phys. Rev. B **83**, 214519 (2011).
- [75] M Yi, D. H. Lu, R. G. Moore, K. Kihou, C.-H. Lee, A. Iyo, H. Eisaki, T. Yoshida, A. Fujimori, and Z.-X. Shen, *Electronic reconstruction through the structural and magnetic transitions in detwinned NaFeAs*, New J. Phys. **14**, 073019 (2012).
- [76] J. M. Caron, J. R. Neilson, D. C. Miller, K. Arpino, A. Llobet, and T. M. McQueen, *Orbital-selective magnetism in the spin-ladder iron selenides Ba_{1-x}K_xFe₂Se₃*, Phys. Rev. B **85**, 180405 (2012).
- [77] Julián Rincón, Adriana Moreo, Gonzalo Alvarez, and Elbio Dagotto, *Exotic Magnetic Order in the Orbital-Selective Mott Regime of Multiorbital Systems*, Phys. Rev. Lett. **112**, 106405 (2014).
- [78] M. Mourigal, Shan Wu, M. B. Stone, J. R. Neilson, J. M. Caron, T. M. McQueen, and C. L. Broholm, *Block Magnetic Excitations in the Orbitaly Selective Mott Insulator BaFe₂Se₃*, Phys. Rev. Lett. **115**, 047401 (2015).
- [79] Seulki Roh, Soohyeon Shin, Jaekyung Jang, Seokbae Lee, Myoungsoon Lee, Yu-Seong Seo, Weiwu Li, Tobias Biesner, Martin Dressel, Joo Yull Rhee, Tuson Park, and Jungseok Hwang, *Magnetic-order-driven metal-insulator transitions in the quasi-one-dimensional spin-ladder compounds BaFe₂S₃ and BaFe₂Se₃*, Phys. Rev. B **101**, 115118 (2020).
- [80] Qing Li, Guixin Cao, Satoshi Okamoto, Jieyu Yi, Wenzhi Lin, Brian C. Sales, Jiaqiang Yan, Ryotaro Arita, Jan Kuneš, Anton V. Kozhevnikov, Adolfo G. Eguluz, Masatoshi Imada, Zheng Gai, Minghu Pan, and David G. Mandrus, *Atomically resolved spectroscopic study of Sr₂IrO₄: Experiment and theory*, Sci. Rep. **3**, 3073 (2013). <https://doi.org/10.1038/srep03073>
- [81] A. Yamasaki *et al.*, *Bulk nature of layered perovskite iridates beyond the Mott scenario: An approach from a bulk-sensitive photoemission study*, Phys. Rev. B **89**, 121111(R) (2014).
- [82] Hiroshi Watanabe, Tomonori Shirakawa, and Seiji Yunoki, *Theoretical study of insulating mechanism in multiorbital Hubbard models with a large spin-orbit coupling: Slater versus Mott scenario in Sr₂IrO₄*, Phys. Rev. B **89**, 165115 (2014).
- [83] M. Nakayama, Takeshi Kondo, Z. Tian, J. J. Ishikawa, M. Halim, C. Bareille, W. Malaeb, K. Kuroda, T. Tomita, S. Ideta, K. Tanaka, M. Matsunami, S. Kimura, N. Inami, K. Ono, H. Kumigashira, L. Balents, S. Nakatsuji, and S. Shin, *Slater to Mott Crossover in the Metal to Insulator Transition of Nd₂Ir₂O₇*, Phys. Rev. Lett. **117**, 056403 (2016).
- [84] I. R. Fisher, L. Degiorgi, and Z.-X. Shen, *In-plane electronic anisotropy of underdoped '122' Fe-arsenide superconductors revealed by measurements of detwinned single crystals*, Rep. Prog. Phys. **74**, 12 (2011).